An Overview of CVD Diamond Growth on Ceramics and Synthesis of CNTs at the University of Aveiro

Eduardo Silva[1], Sérgio Pratas[1], Aneeta Jaggernauth[1], Ricardo Silva[1], Miguel Neto[1], Filipe Oliveira[1], Rui Silva[1]

[1] CICECO - Aveiro Institute of Materials, Departament of Materials and Ceramic Engineering, University of Aveiro, 3810-193 Aveiro, Portugal

The Carbon and Ceramic Composites Group from the University of Aveiro has been active for almost 25 years, working mostly on applied research. Led by Professor Rui Silva, it all started with a study about the wear properties of tungsten carbide coated CVD diamond [1]. Since then, diamond coatings synthesized by hot filament assisted chemical vapour deposition (HFCVD) became the core developed material both for machining and biological applications, especially due to the simultaneous development of a special silicon nitride (Si_3N_4) composition, an outstanding substrate for CVD diamond coatings due to the strong bonding between both materials. This dual system has found its most notable performance in cutting tools and hip joint prosthetics.

Along with the nanomaterials revolution, the group didn't fall behind and started working on the CVD synthesis of carbon nanotubes (CNTs) as materials with bone growth stimulation properties, and later on, as core electrode materials for electrochemical capacitors. The research on CVD diamond also went a step forward. By doping diamond with boron, it could be used as a semiconducting material, which in combination with its intrinsic chemical inertness, biocompatibility and mechanical robustness, could yield sensors with unique properties for biological and corrosion related applications.

This group along with other colleagues from the University of Aveiro has placed Portugal in the map of CVD diamond research, making it the 15th country worldwide with most published articles on the topic. This has only been possible through the networking efforts and expertise of Prof. Rui Silva and Dr. Filipe Oliveira, along with the ability to fabricate in-house HFCVD reactors, mostly through the skills of Dr. Miguel Neto. The innovation towards higher-end applications such as biosensors and smart regenerative materials didn't stay behind closed doors. By focusing on applied research, the Carbon and Ceramic Composites Group has also contributed for the development of the regional economy through the many partnerships with local industries.

In the following pages, we present a brief overview of the most relevant work that our group has been developing in recent years.

Diamond coatings by HFCVD for tribological applications

Mostly known for great beauty and high value, diamond is a much more important and useful material in a form and scale that departs from the shiny crystals that people tend to admire. Chemical vapor deposition (CVD) is one of the techniques that allow the synthesis of diamond coatings. These are polycrystalline layers where diamond crystallites within the micro- to nanometer range are bound together and can be grown in the form of well adherent and homogeneous coatings. CVD diamond coatings exhibit unique properties such as extreme hardness and thermal conductivity, as well as chemical inertness. These properties make them ideal for harsh mechanical and/or chemical conditions, such as cutting of highly abrasive materials and mechanical seals for pumping of corrosive liquids [2].

H_2 and CH_4 are the most commonly used gas species for diamond growth by hot filament-assisted CVD. The gases require activation, which can be thermally assisted by hot wires at low pressure ranging roughly from 20 to 200 mbar. Following the activation step, the radicals are transported to a previously seeded substrate where diffusion of species occurs. At the growing surface, the hydrogen abstraction reaction is very important to promote the substitution of atomic hydrogen by methyl radicals, resulting in the growth of diamond crystals (Figure 1). Carbide forming substrates are preferred for the growth of CVD diamond, to improve mechanical adhesion, among other reasons. As a pre-conditioning step, substrates are "seeded" with diamond particles that create preferential nucleation spots. The morphology of diamond crystals can be controlled by proper parameter adjustment on the CVD system, allowing the crystallite size to vary within the micrometer to nanometer range (Figure 1).

While microcrystalline diamond (MCD) exhibits overall better adhesion to substrates, its surface is also rougher, which can be a disadvantage. On the other size range, nanocrystalline diamond (NCD) exhibits a much smoother surface but its adhesion is inferior. A typical route to grow nanodiamond crystals is to promote renucleation. Under such conditions, diamond crystals do not grow in the typical columnar structure of MCD, with large crystals, giving place to agglomerates of densely packed diamond nanocrystals instead [32,33].

Adhesion and wear rate are two of the most critical aspects governing the performance and cost/benefit relation of CVD diamond coatings. With this in mind, our group has developed a series of important works in the field of CVD diamond tribology, mainly concerning their application for machining, mechanical seals and biotechnology.

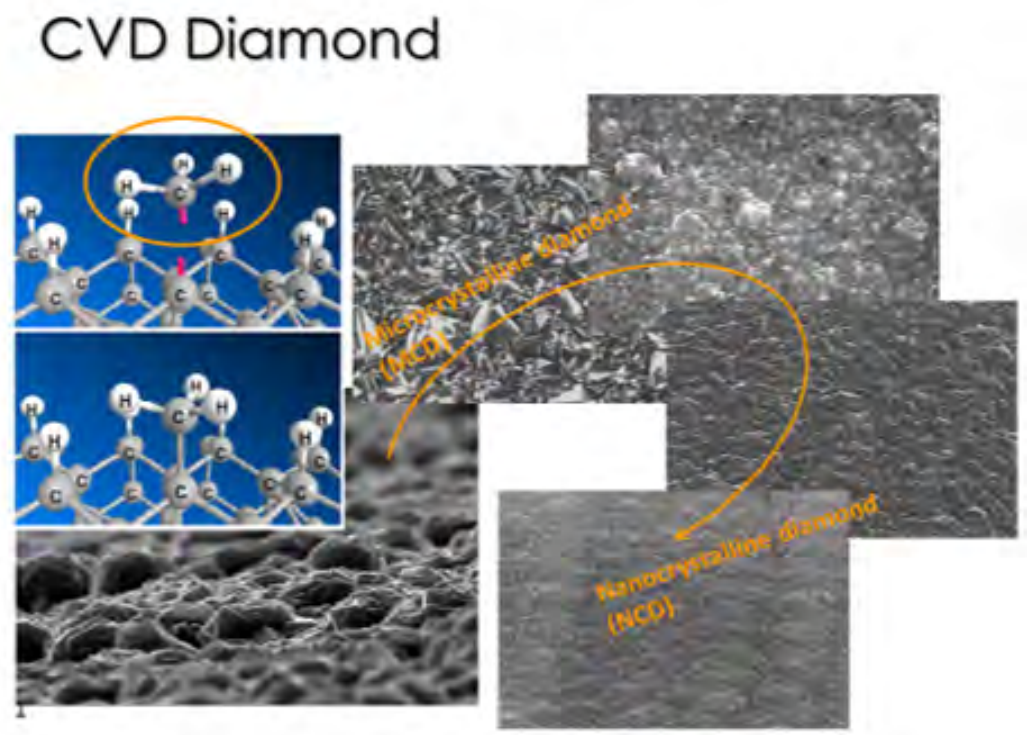

Figure 1. Growth mechanism and the different morphologies of CVD diamond.

Flávia Almeida was one of the main contributors in this regard, presenting works about the tribological properties and machining performance of CVD diamond coatings on Si_3N_4 and hard metal (WC-Co, or cemented carbide) substrates. In [3] the adhesion of different diamond morphologies to Si3N4 substrates was evaluated with the objective of optimizing the properties of nanocrystalline diamond, especially adhesion. Three different morphologies were synthesized by hot filament assisted CVD and studied: microcrystalline (MCD), submicrocrystalline (SMCD) and nanocrystalline diamond (NCD). Although all morphologies showed good adhesion, MCD registered the highest. It was found that pre-treating the Si_3N_4 substrates with CF4 plasma provided an enhanced mechanical interlocking at the matrix/coating interface. The MCD film showed highest adhesion, supporting a normal load of 1600 N without peeling-off, with an interfacial crack resistance of 12.0 N μm^{-1}. This represented a significant advance in adhesion level for the referred system. The highest adhesion exhibited by MCD in comparison to SMCD and NCD was attributed to less amount of graphitic phase at the interface, which enabled a stronger bonding to Si_3N_4.

In fact, in a dedicated interfacial study by HRTEM and HRSEM-EELS analysis, the high adhesion levels of MCD were attributed to the spontaneous growth of DLC (Diamond-Like Carbon) interlayers, which relax the thermal residual stress in the interfacial region [4]. These layers are intercalated with diamond direct nucleation regions exhibiting grain-to-grain epitaxial growth.

Despite its superior bonding, MCD is hardly a choice in certain applications due to its characteristic high roughness, due to the micro-sized pyramidal asperities of diamond crystals, which lead to mechanical interlocking [5]. Consequently, high initial friction values in sliding contacts are observed leading to higher stress levels, temperature and ultimately to the increase in the wear rate [6]. Hence NCD represents a better solution, especially for sliding surfaces under high load. A work from Cristiano Abreu showed that NCD on NCD tribopairs under water lubrication led to very mild to mild wear regimes, with the wear coefficient values varying from 10^{-9} to 10^{-8} mm3$N^{-1}m^{-1}$ [7].

Diamond coatings were also investigated for the turning of hardmetal, a process which provides energy savings and better finishing quality that wheel grinding [8]. While polycrystalline diamond and polycrystalline cubic boron nitride are the standard materials for this process, Almeida has demonstrated that CVD diamond coated hardmetal tools enabled a much better performance than PCD (Polycrystalline Diamond) and PCBN (Polycrystalline Cubic Boron Nitride) ones, leading to much lower wear rates and higher tool durability [8]. While the friction coefficient between the chip and rake face reached values of 0.6–0.7 for the CVD tools after 180 m, the PCD one attained the same 0.7 coefficient value after mere 70 m. Moreover, it was found that the PCD tool also had a larger amount of adhered workpiece material than the CVD ones, which was caused by the chemical affinity of common Co binder in the PCD tool and the hardmetal workpiece.

In another report, further investigation and comparison between uncoated and NCD coated drill bits showed a remarkably superior performance of the later tools in drilling of pre-sintered cemented carbide (WC-5.5 wt.% Co) [9]. While the bare hardmetal drill bit exhibited a low infeed rate (20 mm/min) and increase of axial force from 4 to 20 N after four holes, the NCD-coated hardmetal tool allowed for infeed rates of 940

mm/min, reaching the same axial force of 20 N only at 500 mm/min. All this was done keeping the integrity of the tool and good surface finishing of the resulting hole. But the secret to such high performance of hardmetal tools coated with CVD diamond comes from even before the tools enter the CVD chamber. A two step pre-treatment with Murakami and Aqua regia is used for the purpose of removing cobalt from the surface of hardmetal due to its inhibitory effect on diamond nucleation, promoting formation of graphitic phases instead [10]. With this kind of pre-treatment, diamond seeding, nucleation and anchoring are much more effective, allowing the hardmetal tool to benefit from the intrinsic properties of the diamond coating, without compromising its mechanical integrity.

A more environmentally friendly alternative to acid pre-treatment of hardmetal tools has been recently employed by Sérgio Pratas. Via this route, a tungsten carbide interlayer is formed by means of tungsten vaporization and carburization during 1 hour (i.e. saturation of the hardmetal surface with a high CH4/H2 ratio of thermally activated gas) (Figure 2). After this period the pretended diamond synthesis parameters are introduced and the growth begins. As a result of this one-step solution, diamond films with high adherence can be produced, thanks to the absence of graphite at the harmetal/diamond interface.

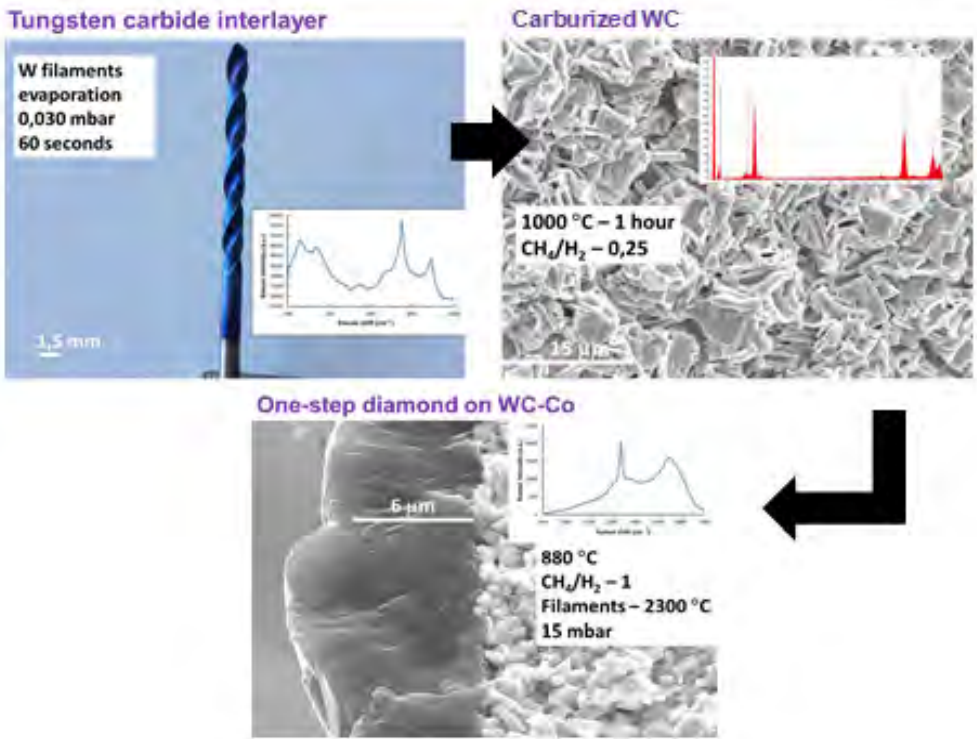

Figure 2. Growth procedure for CVD diamond on WC-Co with tungsten carbide interlayer.

By now it is clear that NCD is an excelling coating for more efficient tools and tribological systems because it is smooth, while still providing high hardness and low wear rate. However, it is also clear that MCD provides for higher adhesion due to better bonding at the interface. In order to combine the advantages of both morphologies, Ermelinda Salgueiredo has investigated the behaviour of multilayer diamond coatings [11]. Besides the above-mentioned advantages, multilayer diamond coatings were developed with two main goals: to mitigate catastrophic crack propagation, typical of ceramic materials, and to take advantage of NCD for stress relieving within the coating. Single, bilayer and multilayer coatings were compared. In order to evaluate adhesion and fracture propagation mode, the coatings were submitted to sandblasting with SiC particles. For single MCD and NCD layers, it was found that a substrate (Si3N4) pre-conditioning step of CF4 plasma attack plus flat lapping with diamond suspension was vital to transition from catastrophic and extensive delamination of the coatings, to more localized removal of smaller parts of the coatings. For the multilayered ones, under sandblasting with SiC particles, the tests were stopped after more than two hours without any signal of extensive delamination [11]. Damage occurred only by gradual loosening of material from the surface. A stress field distribution model was developed in order to characterize the different behaviour of the multilayered diamond coatings. According to this model, the maximum value of the von Mises parameter J21/2 is found at MCD/NCD interfaces. Crack propagation occurs along this region, working as a toughening mechanism by absorbing impact energy of SiC particles, and ultimately delaying delamination of the coatings.

The transitory interfaces between diamond layers on multilayer coatings have been investigated by HRTEM (High Resolution Transmission Electron Microscopy), STEM-EDX (Scanning Transmission Electron Microscopy – Energy Dispersive X-Ray Spectroscopy), and EELS (Electron Energy Loss Spectroscopy) [12]. This study showed that the

nature of the interface depends on which type of layer is on the base. While for MCD to NCD transitions graphite-like structures where more prominent, (as shown by the π* C peak at 285 eV in spatially resolved STEM-EELS), for NCD to MCD transitions, non-diamond material is absent. This is caused by the new gas composition at the start of a new layer: higher methane and lower hydrogen for NCD and the opposite for MCD. Hence, at the NCD-to-MCD interface graphite could not be detected because it was most likely etched away by atomic hydrogen.

Going a step further, the tribological behaviour of the multilayer architecture was tested on self-mated ball-on-flat setup [6]. Comparison between monolayers, bi- and fourfold multilayers of micro- and nanocrystalline CVD diamond morphologies revealed that none of the tested architectures showed coating delamination on both high-load & short-term tests (max 200 N; 86 m) and endurance tests (60 N; 691 m). The experiments were performed in the absence of lubrication, showing very low values of friction coefficient ranging from 0.02 to 0.09. The four fold multilayer coating with NCD on the top most layer outperformed the coatings with less layers by combining high wear resistance (~2.4×10^{-7} mm3N^{-1} m^{-1}) and a low friction coefficient (0.06) under an applied load of 200 N, without delamination [6]. The top nanocrystalline diamond layer was found to progressively wear out, as a sacrificial layer, while the harder microcrystalline diamond layer underneath kept the residual stresses low.

Such superior performance undoubtedly makes multilayer diamond coatings ideal for highly demanding tribological applications subjected to high contact pressures where lubrication is unpractical, or when low friction coefficient and high wear resistance are mandatory. A practical example of multilayer diamond coatings in action comes from another work of Almeida as leading author. The idea was to investigate the tribological behaviour of bare Si_3N_4, Si_3N_4 coated with micro/nano multilayers of CVD diamond, and AISI 52100 hardened chrome alloy steel [13]. The choice of materials was related to the possible application of CVD diamond in biodiesel lubricated systems. Because of the higher electric conductivity in comparison to petrol-based fuels, biodiesel creates conditions for higher corrosion rates, to which CVD diamond is resistant. As main outcome, this study demonstrated that the friction coefficient (COF) for multilayer diamond is lower than for steel (0.07 vs 0.1) and the wear regimes in lubricated and unlubricated condition are very similar (k~10^{-8} mm3$N^{-1}m^{-1}$) [13]. As for the bare Si3N4 both the friction and wear coefficients proved it unreliable for the considered application, especially in dry condition.

A more recent study was designed to understand the effects of relative humidity (RH), and temperature on the sliding and wear behaviour of multilayer diamond [14]. As mentioned before, the material is suited for high abrasion applications and poor lubrication conditions. The ten-fold multi-layered coating was synthesized on top of Si3N4 by alternating micro- and nanocrystalline diamond layers with A/B/A sequence, starting with MCD for higher adhesion to Si3N4 and ending with a top NCD layer for a smoother surface (Figure 3). Immediately, a difference in the critical indentation load of 600 N for single NCD layer and 900 for the 10-fold multilayer coating was established. Self-mated ball-on-plate tribological tests with RH (10 to 90 %) and temperature (25-100 ºC) as main variables revealed that while the effect of RH on the friction coefficient is minimal, it is very pronounced on the critical load value (load above which the coating detaches), increasing from 40 N at 10% RH to 120 N at 90% [14]. This was explained by the formation of a water layer between the surfaces of the ball and the plate which extends the contact area during sliding, inducing a load bearing effect. The static friction coefficient was observed to increase with temperature, most likely due to lower lubrication induced by the dryer conditions. The effect of temperature on the critical load was very pronounced, ranging from 40 to 55 N within the studied temperature range [14]. Overall the study points out the importance of water as load bearing medium, even for materials that are suitable for operation under low lubrication sliding.

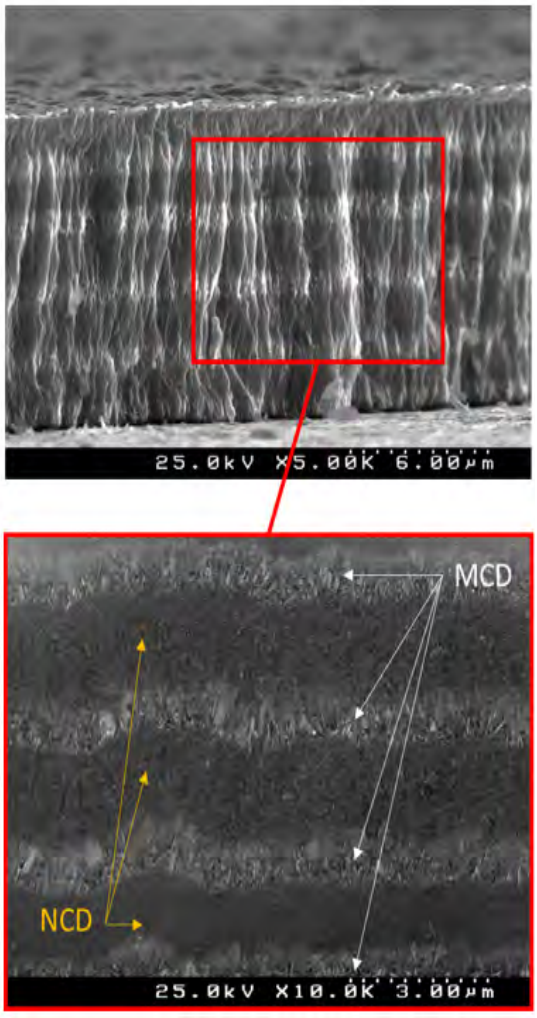

Figure 3. A/B/A multilayer CVD diamond alternanting between MCD and NCD with NCD as finishing layer for a smoother surface.

CVD diamond is not just a super hard, chemically inert and wear resistant material, it is also biocompatible

and a very interesting material for various biotechnology applications [15]. Margarida Amaral has conducted a non-specific cytotoxicity and biocompatibility analysis on NCD with human gingival fibroblast cells, where the typical morphology and cell growth could be reproduced [16]. With osteoblast cells, NCD was found to increase cell proliferation as well as stimulation of markers such as ALP activity and matrix mineralization, in comparison to polystyrene tissue culture plates.

This study open the door for the application of NCD as a coating for implant applications such as articular joint prosthesis for total hip replacement (THR) [17–19]. With the modern days increase of the life expectancy, there is a corresponding increase of THR interventions. Ceramic materials exhibit good biocompatibility in general, especially when compared to metals, for which ion release may cause osteolysis among other effects. While alumina-on-alumina tribopairs are surgeons' first choice for patients younger than 50 years, Si_3N_4 has been demonstrated to considerably excel the fracture toughness of Al_2O_3, which implies lower fracture probability and less chance of implant replacement or readjustment.

Following the group's previous results with NCD, Amaral presented a work describing a new articular joint prosthesis material consisting of NCD coated Si3N4 ceramic hip joints comprising an NCD/ Si3N4 ceramic femoral head working against an NCD/ Si3N4 acetabular liner [18]. After withstanding one million cycles, which correspond to approximately one year of a hypothetical patient's life, this tribosystem exhibited a wear rate of 0.005 mm3 per million cycles in the second half of the test. This was one order of magnitude lower than the best ceramic-on-ceramic hip joints available at the time. Furthermore, the resulting residual amount of debris did not present cytotoxicity. The Raman spectra collected after the tribological testing demonstrated no significant structural transformations of the coating [18].

In the same line of research, Salgueiredo reported on bilayer MCD/NCD coated Si3N4 odontological drill bits to drill a laminated block that mimics the cortical and trabecular bone [20]. Besides the tribological advantage of this system, NCD debris is harmless and the films exhibit a high resistance to bacterial colonization. The produced drill bits presented a superior performance when compared to AISI 420 steel: reduction of the maximum force applied by about four times in the speed range 350–1400 rpm; cooler operation temperature of less ~4ºC; drilling at low spindle speeds (100 rpm); and higher infeed rates (30 mm/min) which is important to reduce to duration of the surgical procedure. More than just numbers, these figures represent a significant reduction of trauma for the patient.

Boron doped diamond

The extreme hardness and thermal conductivity of CVD diamond determine its main application in cutting and anti-wear parts, as also in heat sinks for electronic and optical components. However, CVD diamond can be doped, which widens the range of applications of this material, as it becomes electrically conductive. For a given film thickness, the conductivity of CVD diamond films may vary from 1×10^{-9} $\Omega^{-1}cm^{-1}$, for lightly doped films, to 100 $\Omega^{-1}cm^{-1}$, for heavily doped ones [21]. When heavily doped ([B] > 1×10^{20} atoms/cm^3), CVD diamond becomes a conducting material or even superconducting at sufficient low temperature (~2K) [21,22]. Accordingly, what determines the conductivity value is going to be the doping source, the concentration of the relevant doping element (boron, nitrogen, phosphorus or sulphur) and the location of B atoms within the diamond lattice. Boron doping yields p-type semiconductivity by introducing an acceptor energy level 0.37 eV above the valence band, while nitrogen or phosphorus doping yield n-type semiconduction [21]. While the latter elements have been reported to successfully dope CVD diamond films, boron exhibits higher doping efficiency due to its lower charge carrier activation energy [21].

In our group, a boron doping system was developed, targeting the application of CVD diamond for corrosion-related sensing and biosensing. Miguel Neto pioneered our works with boron doped diamond (BDD) starting from interfacial studies. The author has characterized the surface of BDD films addressing specifically the boron doping setup of used in our group B2O3 mixed in pure ethanol and dragged by argon gas into the reaction chamber [23]. It is generally accepted that CVD diamond surfaces are H-terminated, mainly due to hydrogen rich gas mixture used for its synthesis. However, with oxygen introduced as part of the mixture it was important to characterize the resulting surface, since this element is known to be detrimental to doping efficiency by compensation of boron-introduced electronic holes. Therefore, by X-ray photoelectron spectroscopy (XPS) and water contact angle measurements, the author studied the surface termination of boron doped NCD and MCD coatings grown on silicon nitride (Si3N4) ceramics, via a boron oxide containing solution carried by argon gas. A dependency between the resulting diamond morphology, the flow of argon and the system pressure could be established. Although the water contact angle of ~90º revealed a hydrophobic surface, the XPS characterization revealed that the surface is only partially H-terminated with the remaining area consisting mainly of C–O–C and C=O terminating groups. The experimental data shows that oxygen is not restricted to the surface and may also be incorporated in the film during the CVD process [23].

In a subsequent study, the focus was the development of suitable electrical contacts for the development of BDD based electronic devices [24]. These should possess low electrical resistivity to minimize device losses at the metal–semiconductor interface and they must adhere well to the semiconductor material. The presented solution was the deposition of single-

-phase WC layers, an electrically conducting material, providing high thermal stability at the interface [24]. Diamond was grown uninterruptedly from the interior of the tungsten layer instead of from its surface. The process consisted on vaporizing tungsten oxide (WO_2) from the system's own heating filaments, under vacuum (10^{-2} bar) in a heating range of 1500-1900ºC [24]. The methane used for diamond growth will convert the oxide layer to WC during the first minutes of diamond growth. The success of the entire process was shown to rely on the substrate preconditioning with diamond particle seeding to ensure dense nucleation of the BDD film.

Later on, Neto has demonstrated the synthesis of metal-like boron doped diamond coatings on highly dielectric silicon nitride ceramic substrates [25]. The boron source was boron oxide mixed in ethanol. It was found that doping efficiency increases significantly with higher growth temperature and pressure, as well as lower methane content. Characterization by SIMS (Secondary Ion Mass Spectroscopy) depth profile analysis demonstrated that boron was uniformly distributed throughout the deposited diamond coatings [25]. In the case of NCD, boron was predominantly incorporated in passive electrical sites at the grain boundaries, which compromised the conductivity of the film.

A practical application of diamond as a temperature sensitive coating has been demonstrated in the form of an NTC (negative temperature coefficient) thermistor. The idea was to address the issues of tooth overheating and vitality in dental medicine. The deposition parameters in a HFCVD reactor were optimized for electrical resistance and B parameter using Taguchi's method. The device was assembled by applying in-situ ohmic contacts, isolating with undoped CVD diamond and using a PCB strip for electrical contacts and temperature measurements (Figure 4). The base of a pig molar tooth was placed inside a hot/cool water circuit and the temperature of the exposed surface was measured with the new NTCs. The sensors exhibited fast response time, high thermal sensitivity, while being bio-inert and biocompatible (Figure 5).

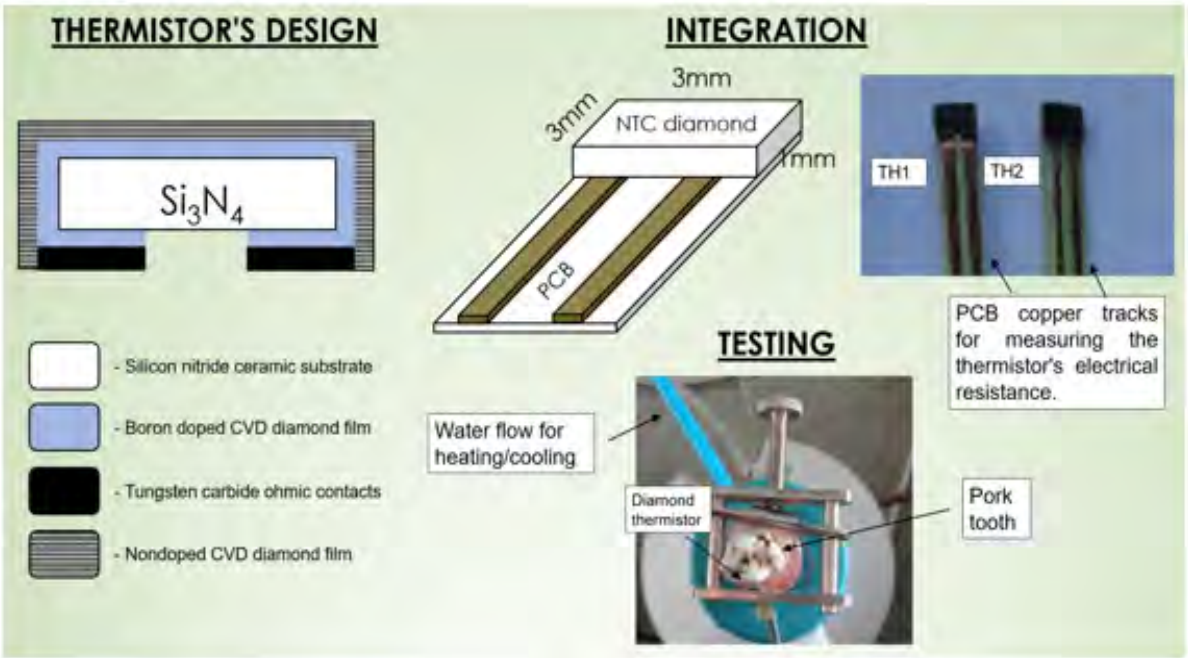

Figure 4. Diamond thermistor design and testing setup.

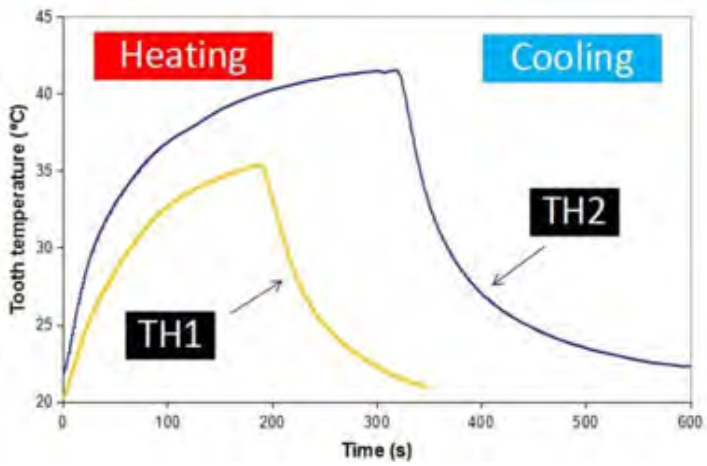

Figure 5. CVD diamond film behavior as NTC thermistor during heating/cooling cycle.

Boron doped diamond (BDD) is also an electrochemically active and functional material. It has gathered the interest of the scientific community due to its unmatched combination of properties: wide electrochemical potential window for water electrolysis, high-signal-to-noise ratio, high chemical stability, resistance to fouling, among others [26]. At a smaller scale Eduardo Silva started developing BDD microelectrodes applied to the field of corrosion, in particular for pH and dissolved oxygen (DO) sensing.

In a recent study BDD microelectrodes were developed as a possible alternative to suppress the limitations of glass membrane and glass capillary microelectrodes based on a selective ionophore-based oil-like membrane [27]. Although they are the standard for pH measurement, especially at the microscale, these electrodes present some disadvantages like spontaneous leakage of the liquid membrane, low mechanical robustness and short life time [28]. Moreover, the sensitivity and selectivity of such electrodes are constrained by adverse effects such as trans-membrane ion fluxes, which change the composition of the sample solution near the membrane, affecting the lower detection limit [29]. pH sensitivity of the microelectrodes was achieved by means of oxygen plasma treatment, after coating sharp tungsten wires with BDD. At this hydrophilic surface differently charged surface groups like C-OH, C-O^- and C-OH_2^+ can form, by a protonation–deprotonation mechanism, depending on the proton concentration in solution. The developed microelectrodes (Figure 6a) exhibited fast response and linearity with 50.8 ± 1.0 mV/pH in a wide range from pH 2 to 12. When tested on a galvanic Zn-Fe couple immersed in 0.05 M NaCl, the BDD microelectrodes successfully allowed mapping the local pH which varied from ~4.8 above the zinc under anodic dissolution and 9.3 over the iron cathodic area [27]. Although not illustrated in the same article, Figure 6b shows the typical behaviour that can be expected by BDD pH sensitive microelectrodes.

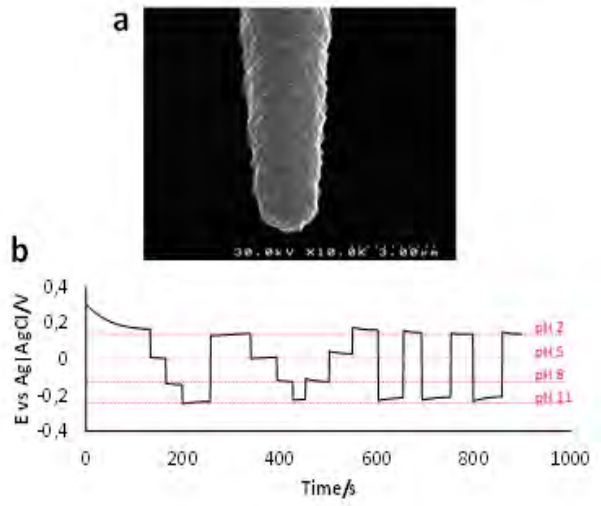

Figure 6. a) BDD pH sensitive microelectrode. b) The recorded potential in different pH solutions, shows a fast and stable response.

In another work, BDD microelectrodes were optimized for the detection of dissolved oxygen (DO) [30]. DO is one of the most important oxidizing species involved in cellular metabolism as well as in microbiological and corrosion processes. In the latter case, DO is the main cathodic reactant at neutral and alkaline pH for most engineering metals and alloys [31]. The development of corrosion protection strategies involves assessing the surface of metals with high degree of spatial resolution, which can be done by techniques such as SVET (Scanning Vibrating Electrode Technique) or microamperometry. The developed BDD microelectrodes were submitted to a surface modification with CF_4 plasma, which enabled high sensitivity to DO, by means of complexation with surface fluorine groups and electrochemical reduction [30]. A model galvanic cell immersed in aqueous electrolyte was used as setup for DO detection by using a SVET system in the amperometric mode (Figure 7a). It was demonstrated that BDD microelectrodes exhibited fast response and a detection limit of 0.63 µM. When scanning the near-surface of the model galvanic cell, the measured DO followed the expected distribution. Accordingly, the oxygen concentration was lower above the cathodic area, which is to expect since it is consumed mainly at the cathode (Figure 7b).

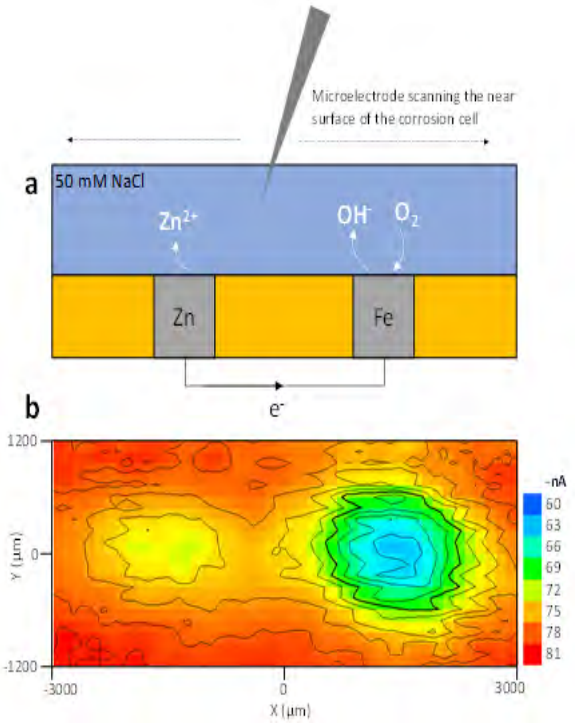

Figure 7. a) Model galvanic Zn-Fe system. b) DO oxygen map recorded with a BDD microelectrode. Less negative currents mean higher DO depletion. Since there is less oxygen available above the iron cathode, this is translated into lower DO reduction current at the BDD microelectrode.

Among the most relevant aspects of microelectrode construction is the choice for its geometry, which is related to the size tolerable for application, and needs to be dimensionally well defined, for analyte quantification purposes. A defective or irregular insulating shroud can give origin to the misinterpretation of electrochemical data. An alternative to insulation

with polymeric coatings has been presented by Silva: boron doped diamond microelectrodes insulated with undoped diamond [32]. Upon FIB (Focused Ion Beam) cutting, chemically and dimensionally stable all-diamond microelectrodes were obtained. A central, electroactive disk (BDD) insulated by a thin undoped diamond coating. This concept was demonstrated for local oxygen measurements on the Al–Cu–CFRP (Carbon Fiber Reinforced Polymer) system, which is of high relevance for the development of new composite materials for the aeronautics industry.

CNTs and hybrid materials

Asides from diamond, CVD synthesis of carbon nanotubes have been investigated in our group. It is well known that CNTs have been one of the cornerstones of the nanotechnology revolution worldwide. Due to their low cost and supreme electrical, mechanical and optical properties these rolled graphene sheets have been attracting a lot of scientific and industrial interest from sectors such as biotechnology for drug delivery and in vitro diagnosis, to energy production and storage, as high surface area electrodes or supercapacitors [33,34]. With several thousands of tons of produced worldwide, CNTs are finding their way to real world widespread usage, although limitations still persist, such as precisely controlling orientation and chirality. Diogo Mata was the first author to focus on CNT based materials, directing most of his endeavors to biotechnology. Endogenous electric signals are involved in the regeneration mechanism of bone through activation of Ca^{2+} channels located in the plasma membrane of osteoblasts. In the case of injury, the electric signals are disrupted. Accordingly, several authors reported accelerated bone regeneration when stimulated by electrically conductive composite bone grafts. In comparison with metal fillers, CNT do not exhibit corrosion-related toxicological risks, while still having high electric conductivity (~100 $S.m^{-1}$) at low percolation values of 0.6–3.5 vol.% [35]. In one of his works with smart CNT-based bone grafts, Mata reported on the development of CNT/HA/glass composites, focusing on the optimization of their mechanical, electrical and cytotoxic behaviour [36]. Comparing with non-electrically stimulated HA/glass matrix, it was demonstrated that the addition of CNTs enabled an increase in the cellular metabolic activity and DNA content of 130% and 60%, respectively, after only 3 days of daily stimulation of 15 μA for 15 min. Furthermore, the osteoblastic gene expression for Runx2, OC and ALP was enhanced by 80%, 50% and 25%, respectively, after 5 days of stimulation [36]. Such improvement in the functional activity of osteoblast cells were directly related to the local increase in the culture medium conductivity and the ability to apply confined electrical stimulate.

Although this work successfully demonstrated the viability of smart CNT-based bone grafts, the toxicological aspects of CNTs have been a matter of dispute for a long time. Metal impurities, tube morphology, hydrophobicity and non-biodegradability are mostly responsible for the toxicological profiles of CNTs. While transition-metal impurities (used as catalysts for CNT production) may induce cellular oxidative stress, the morphology of CNTs is responsible for the success of clearance, by means of the urinary and/or lymphatic systems [37]. However, even CNTs with proper size, dispersion and purity may still present cytotoxicity, due to hydrophobicity and biopersistency [38]. This can be solved by means of chemical functionalization that restricts CNT agglomeration and increases their mobility in physiological serums, avoiding accumulation in tissues and organs [37]. The functionalization of multi-walled carbon nanotube (MWCNTs) membranes by the [4 + 2] Diels–Alder cycloaddition reaction of 1,3 butadiene has been studied by Mata and co-workers in terms of functionalization yield, functional groups recognition, surface charge, wettability and roughness [39]. The biocompatibility and biodegradability of Diels–Alder functionalized CNT membranes were assessed in vitro with human-like osteoblasts and in vivo through implantation in Wister rats. While both functionalized and non-functionalized CNTs demonstrated adequate cell adhesion, enhanced cell spreading was observed for the functionalized ones [39]. This behaviour was attributed to the difference in surface energy, which also marked the improved proliferation and osteogenic differentiation, supported by higher MTT reduction values and ALP activity values, for the functionalized CNT membranes. When implanted in the Wistar rats, the Diels-Alder functionalized membranes induced less inflammatory response than their non-functionalized counterpart, as well as improved biodegradation [39]. Hence, this report demonstrated that cycloaddition reactions provide an optimal balance between preservation of CNT properties and in vivo biodegradability, providing a suitable route for bone healing modulation.

Although Mata has also developed fabrication approaches for smart bone grafts [26], perhaps the most innovative work regarding this topic was presented by Elsa Gonçalves. The author studied the behaviour of a 3D printed composite scaffold composed of silicon-doped nanocrystalline hydroxyapatite (HA) (similar composition to bone with better biological response), polycaprolactone (biodegradable polymer), and carbon nanotubes (to improve mechanical properties and electrical conductivity) [42]. The outcome of this rapid prototyping process was a composite with homogeneous distribution of HA and CNTs on a porous PCL (Polycaprolactone) matrix. An optimal CNT loading of 2% wt. was found to make the composite conductive and exhibit a compressive strength of 4 MPa, which is similar to trabecular bone. Increasing the CNT load to 10% wt. resulted in better cell adhesion due to improved protein adsorption [42].

In comparison to horizontally aligned CNTs and agglomerates, vertically aligned carbon nanotubes (VACNTs) enable the maximization of the intrinsic properties of CNTs, providing a fully accessible surface area, high electrical conductivity and ballistic

mass transport through tube porosity, along with high mechanical, chemical, and electrochemical stability. Other characteristics of VACNTs include growth with residual amorphous carbon (or none at all) and low amount of catalyst. This CNT morphology leads to the realization of the most noticeable proposed applications of this unique material such as supercapacitors, advanced yarns and fabrics, electronic interconnects, among many others [43].

In our group Ricardo Silva, is currently the main author developing VACNT based materials. In one of his works the author stressed the importance of growing VACNTs directly on metallic substrates (Inconel600). However, there is an obvious limitation to this procedure: diffusion of the catalyst particles that are required for CNT growth into the metal substrate. Hence a typical synthesis by CVD either involves a two-step process of growing VACNTs independently and then bind them to a metal collector or using an oxide buffer layer between the metal substrate and the catalyst particles. Either of the two is problematic because good electrical contact between the VACNTs and the metal substrate is required for optimal performance. The presented solution was annealing of the Inconel600 alloy in air, which led to the formation of uniformly dispersed and densely packed nano-sized catalytic particles (Figure 8) [44]. Hence, the metallic substrate plays two key roles: (i) the Inconel600 itself provides catalytic active sites for the nanotube growth process and (ii) acts as a current collector. This formation of catalyst particles in situ directly from the Inconel substrate, allows the successful growth of VACNTs with excellent adhesion and electrical contact [44].

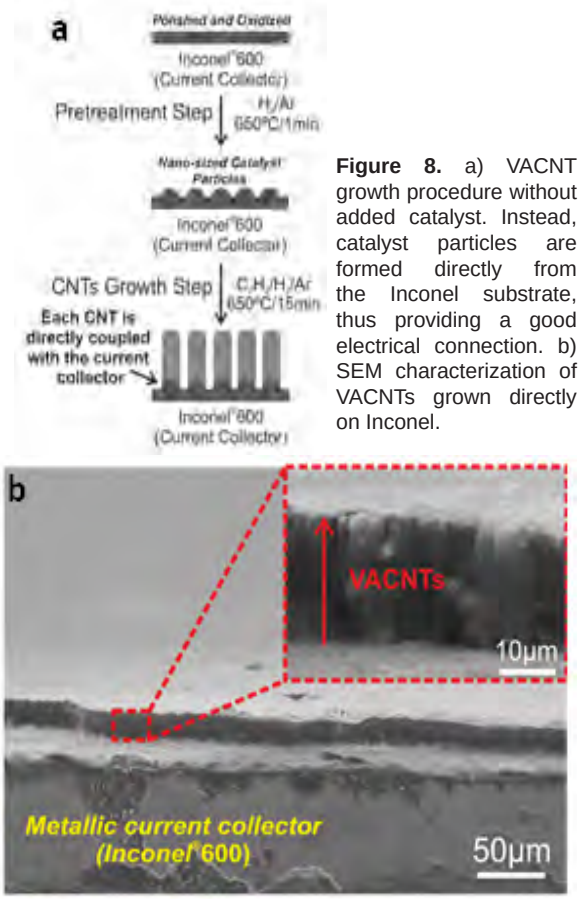

Figure 8. a) VACNT growth procedure without added catalyst. Instead, catalyst particles are formed directly from the Inconel substrate, thus providing a good electrical connection. b) SEM characterization of VACNTs grown directly on Inconel.

Other scientific contributions from the author include the development of novel hybrid materials for supercapacitors, particularly coating VACNTs with transition metal oxides by atomic layer deposition (ALD). An example of such approach was the coating of VACNTs with manganese oxide by ALD [45]. Electrochemical capacitors can generally be divided in two types: double layer capacitors and pseudocapacitors. While in the first type the capacitance is provided by the charge separation at the electrode–electrolyte interface, in the case of pseudocapacitors it has its origin in fast and reversible Faradaic redox reactions taking place at the electrode. Manganese oxide is very attractive as pseudocapacitor because it presents high theoretical capacitance and low environmental impact. The VACNTs were grown on Inconel600 through the catalyst free process mentioned above, while manganese oxide was deposited by ALD from MeCpMn(I)(CO)3 and O3 as the sources for manganese and oxygen, respectively (Figure 9). As a hybrid material, the VACNTs/Mn3O4 exhibited a synergistic effect, yielding enhanced capacitance for the pair, as compared with pristine VACNTs (Figure 10). The specific capacitance was observed to increase with the number of ALD cycles of Mn_3O_4 (i.e. the thickness of the coating) up to 78.62 $mF.cm^{-2}$, which demonstrates the pseudocapacitive contribution of the Mn_3O_4 in increasing the total capacitance of the nanocomposite [45].

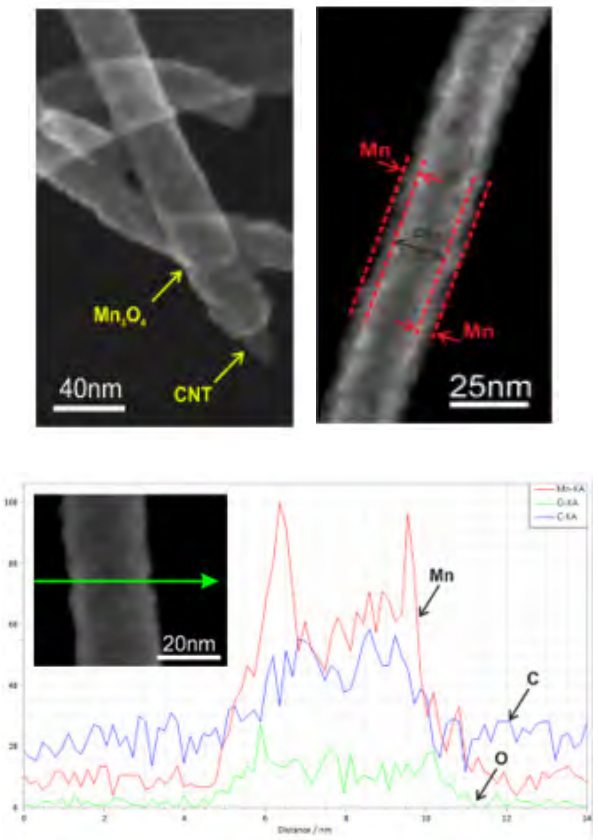

Figure 9. STEM images and corresponding EDS characterization of Mn3O4 coated CNTs, showing a core-shell configuration.

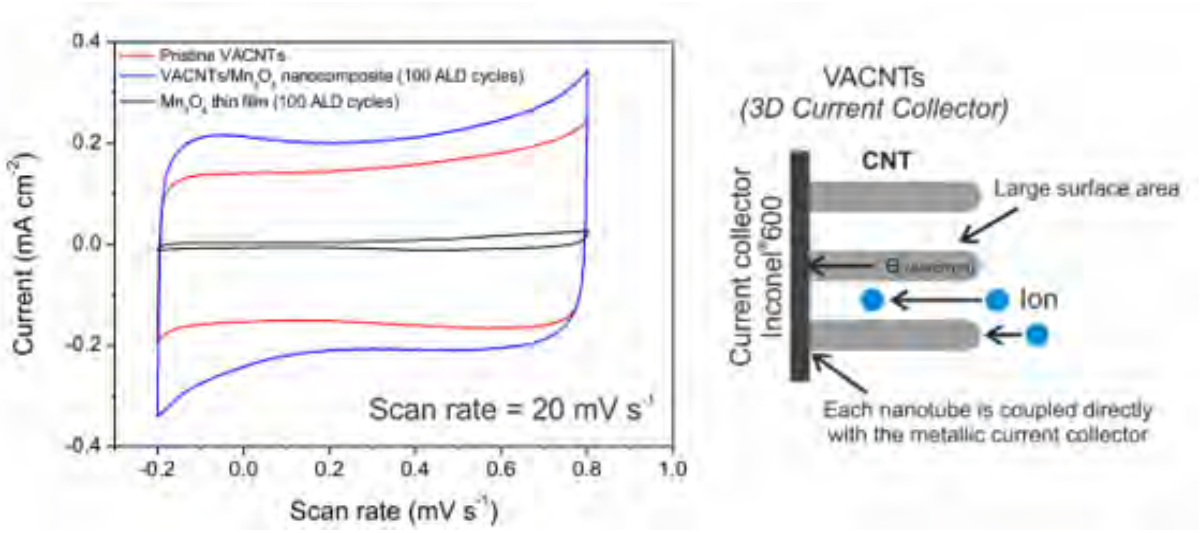

Figure 10. Voltammetric behavior of the VACNTs/Mn3O4 nanocomposite showing a significant capacitance increase for the Mn3O4 coated VACNTs.

The versatility of ALD was used in combination with CVD diamond as well. This study is being developed by Aneeta Jaggernauth. The focus is to take advantage of the high thermal conductivity, high breakdown field and chemical inertness of boron doped diamond for electronic devices operating under extreme or harsh conditions. Challenges of transistors, for example, include high leakage currents and low capacitive coupling between the transistor gate contact and the semiconductor itself. The incorporation of high-κ dielectric materials both as gate insulator and passivation layer on the semiconductor surface, accomplishes surface stability, charge carrier concentration and leakage current minimization. One such high-κ material is Al_2O_3 which is shown in Figure 11 grown by ALD on BDD, with the final goal being the assembly of even higher κ nanolaminates with HfO_2 and Ta_2O_5 deposited on BDD via atomic layer deposition (ALD) for enhanced transistor performance on high power devices and under high temperature conditions.

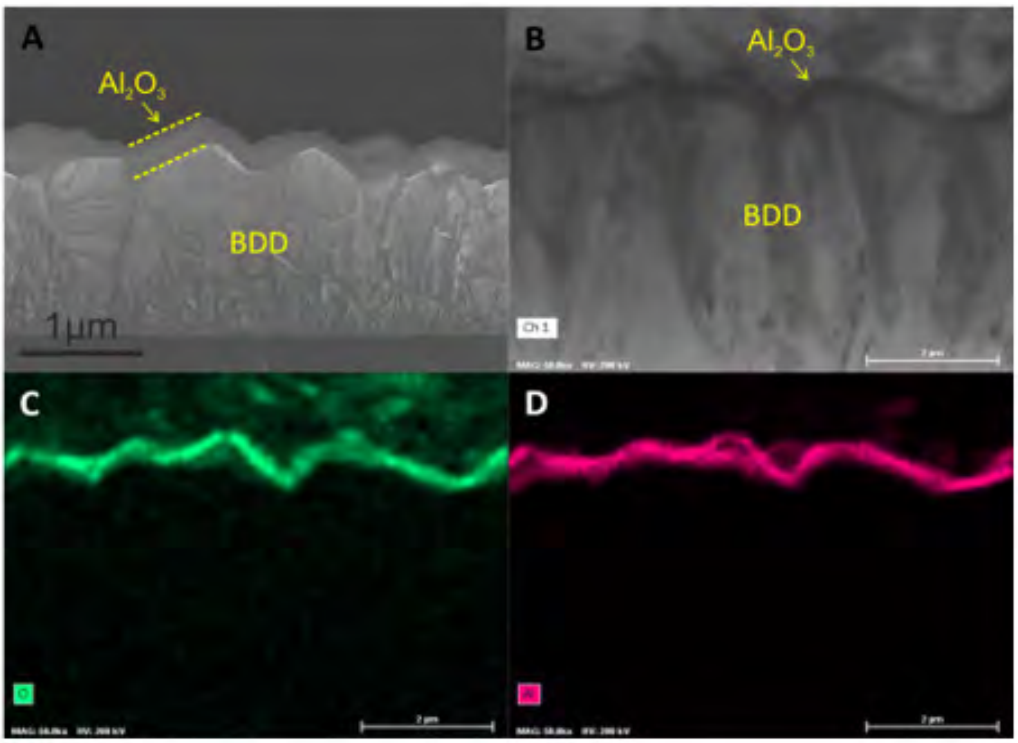

Figure 11. Boron doped diamond coated with Al2O3 by ALD; SEM image shown in A, TEM images in B, C & D with elemental analysis.

References

[1] N.M. Everitt, R.F. Silva, J. Vieira, C.A. Rego, C.R. Henderson, P.W. May, Diam. Relat. Mater. 4 (1995) 730–734.

[2] R.S. Balmer, J.R. Brandon, S.L. Clewes, H.K. Dhillon, J.M. Dodson, I. Friel, P.N. Inglis, T.D. Madgwick, M.L. Markham, T.P. Mollart, N. Perkins, G.A. Scarsbrook, D.J. Twitchen, A.J. Whitehead, J.J. Wilman, S.M. Woollard, J. Phys. Condens. Matter 21 (2009).

[3] F.A. Almeida, M. Amaral, F.J. Oliveira, A.J.S. Fernandes,

R.F. Silva, Vacuum 81 (2007) 1443–1447.

[4] F.A. Almeida, F.J. Oliveira, R.F. Silva, D.L. Baptista, S.B. Peripolli, C.A. Achete, Appl. Phys. Lett. 98 (2011) 1–4.

[5] E. Salgueiredo, M. Amaral, F.A. Almeida, A.J.S. Fernandes, F.J. Oliveira, R.F. Silva, Surf. Coatings Technol. 236 (2013) 380–387.

[6] E. Salgueiredo, C.S. Abreu, M. Amaral, F.J. Oliveira, J.R. Gomes, R.F. Silva, Wear 303 (2013) 225–234.

[7] C.S. Abreu, M. Amaral, F.J. Oliveira, J.R. Gomes, R.F. Silva, Diam. Relat. Mater. 18 (2009) 271–275.

[8] F.A. Almeida, A.J.S. Fernandes, F.J. Oliveira, R.F. Silva, Vacuum 83 (2009) 1218–1223.

[9] F.A. Almeida, J.M. Carrapichano, A.J.S. Fernandes, J. Sacramento, R.F. Silva, F.J. Oliveira, Int. J. Refract. Met. Hard Mater. 29 (2011) 618–622.

[10] F.A. Almeida, E. Soares, A.J.S. Fernandes, J. Sacramento, R.F. Silva, F.J. Oliveira, Vacuum 85 (2011) 1135–1139.

[11] E. Salgueiredo, F.A. Almeida, M. Amaral, M.A. Neto, F.J. Oliveira, R.F. Silva, Wear 297 (2013) 1064–1073.

[12] F.A. Almeida, E. Salgueiredo, F.J. Oliveira, R.F. Silva, D.L. Baptista, S.B. Peripolli, C.A. Achete, ACS Appl. Mater. Interfaces 5 (2013) 11725–11729.

[13] F.A. Almeida, M.M. Maru, M. Shabani, F.J. Oliveira, R.F. Silva, C.A. Achete, Wear 302 (2013) 1370–1377.

[14] M. Shabani, A. C.S., G. J.R., R.F. Silva, O. F.J., Diam. Relat. Mater. 73 (2017) 190–198.

[15] M. Amaral, C.S. Abreu, A.J.S. Fernandes, F.J. Oliveira, J.R. Gomes, R.F. Silva, Surf. Coatings Technol. 204 (2010) 1962–1969.

[16] M. Amaral, P.S. Gomes, M.A. Lopes, J.D. Santos, R.F. Silva, M.H. Fernandes, J. Nanomater. 2008 (2008).

[17] M. Amaral, C.S. Abreu, F.J. Oliveira, J.R. Gomes, R.F. Silva, Diam. Relat. Mater. 17 (2008) 848–852.

[18] M. Amaral, M.M. Maru, S.P. Rodrigues, C.P. Gouvêa, R.M. Trommer, F.J. Oliveira, C.A. Achete, R.F. Silva, Tribol. Int. 89 (2015) 72–77.

[19] M.M. Maru, M. Amaral, S.P. Rodrigues, R. Santos, C.P. Gouvea, B.S. Archanjo, R.M. Trommer, F.J. Oliveira, R.F. Silva, C.A. Achete, J. Mech. Behav. Biomed. Mater. 49 (2015) 175–185.

[20] E. Salgueiredo, F.A. Almeida, M. Amaral, A.J.S. Fernandes, F.M. Costa, R.F. Silva, F.J. Oliveira, Diam. Relat. Mater. 18 (2009) 264–270.

[21] A. Kraft, Int. J. Electrochem. Sci. 2 (2007) 355–385.

[22] W. Gajewski, P. Achatz, O.A. Williams, K. Haenen, E. Bustarret, M. Stutzmann, J.A. Garrido, Phys. Rev. B - Condens. Matter Mater. Phys. 79 (2009) 1–14.

[23] M.A. Neto, G. Pato, N. Bundaleski, O.M.N.D. Teodoro, A.J.S. Fernandes, F.J. Oliveira, R.F. Silva, Diam. Relat. Mater. 64 (2016) 89–96.

[24] M.A. Neto, E.L. Silva, A.J.S. Fernandes, F.J. Oliveira, R.F. Silva, Surf. Coatings Technol. 206 (2012) 3055–3063.

[25] M.A. Neto, E.L. Silva, C.A. Ghumman, O.M. Teodoro, A.J.S. Fernandes, F.J. Oliveira, R.F. Silva, Thin Solid Films 520 (2012) 5260–5266.

[26] N. Yang, S. Yu, J. V. MacPherson, Y. Einaga, H. Zhao, G. Zhao, G.M. Swain, X. Jiang, Chem. Soc. Rev. 48 (2019) 157–204.

[27] E.L. Silva, A.C. Bastos, M.A. Neto, R.F. Silva, M.G.S. Ferreira, M.L. Zheludkevich, F.J. Oliveira, Electrochem. Commun. 40 (2014) 31–34.

[28] D. Amman, Ion-Selective Micro-Electrodes, Principles, Design and Application, Springer-Verlag, 1986.

[29] T. Sokalski, A. Ceresa, T. Zwickl, E. Pretsch, J. Am. Chem. Soc. 119 (1997) 11347–11348.

[30] E. Silva, A.C. Bastos, M. Neto, A.J. Fernandes, R. Silva, M.G.S. Ferreira, M. Zheludkevich, F. Oliveira, Sensors Actuators, B Chem. 204 (2014) 544–551.

[31] E.E. Stansbury, R.A. Buchanan, Fundamentals of Electrochemical Corrosion, ASM International, 2000.

[32] E.L. Silva, C.P. Gouvêa, M.C. Quevedo, M.A. Neto, B.S. Archanjo, A.J.S. Fernandes, C.A. Achete, R.F. Silva, M.L. Zheludkevich, F.J. Oliveira, Anal. Chem. 87 (2015) 6487–6492.

[33] R.H. Baughman, A.A. Zakhidov, W.A. De Heer, Science (80-.). 297 (2002) 787–792.

[34] P. Simon, Y. Gogotsi, Nat. Mater. (2008) 845–854.

[35] J. Tatami, T. Katashima, K. Komeya, T. Meguro, T. Wakihara, J. Am. Ceram. Soc. 88 (2005) 2889–2893.

[36] D. Mata, F.J. Oliveira, M.A. Neto, M. Belmonte, A.C. Bastos, M.A. Lopes, P.S. Gomes, M.H. Fernandes, R.F. Silva, J. Mater. Chem. B 3 (2015) 1831–1845.

[37] L. Lacerda, A. Soundararajan, R. Singh, G. Pastorin, K.T. Al-Jamal, J. Turton, P. Frederik, M.A. Herrero, S. Li, A. Bao, D. Emfietzoglou, S. Mather, W.T. Phillips, M. Prato, A. Bianco, B. Goins, K. Kostarelos, Adv. Mater. 20 (2008) 225–230.

[38] A. Bianco, K. Kostarelos, M. Prato, Chem. Commun. 47 (2011) 10182–10188.

[39] D. Mata, M. Amaral, A.J.S. Fernandes, B. Colaço, A. Gama, M.C. Paiva, P.S. Gomes, R.F. Silva, M.H. Fernandes, Nanoscale 7 (2015) 9238–9251.

[40] D. Mata, F.J. Oliveira, N.M. Ferreira, R.F. Araújo, A.J.S. Fernandes, M.A. Lopes, P.S. Gomes, M.H. Fernandes, R.F. Silva, Nanotechnology 25 (2014).

[41] D. Mata, R.M. Silva, A.J.S. Fernandes, F.J. Oliveira, P.M.F.J. Costa, R.F. Silva, Carbon N. Y. 50 (2012) 3585–3606.

[42] E.M. Gonçalves, F.J. Oliveira, R.F. Silva, M.A. Neto, M.H. Fernandes, M. Amaral, M. Vallet-Regí, M. Vila, J. Biomed. Mater. Res. - Part B Appl. Biomater. 104 (2016) 1210–1219.

[43] W. Shi, D.L. Plata, Green Chem. 20 (2018) 5245–5260.

[44] R.M. Silva, A.C. Bastos, F.J. Oliveira, D.E. Conte, Y. Fan, N. Pinna, R.F. Silva, J. Mater. Chem. A 3 (2015) 17804–17810.

[45] R.M. Silva, G. Clavel, Y. Fan, P. Amsalem, N. Koch, R.F. Silva, N. Pinna, Adv. Mater. Interfaces 3 (2016).